OXFORD

SOT | Society of Toxicology
www.toxsci.oxfordjournals.org

TOXICOLOGICAL SCIENCES, 159(1), 2017, 124–136

doi: 10.1093/toxsci/kfx122
Dryad Digital Repository DOI: http://doi:10.5061/dryad.s05v3
Advance Access Publication Date: June 15, 2017
Research Article

Three-Dimensional (3D) HepaRG Spheroid Model With Physiologically Relevant Xenobiotic Metabolism Competence and Hepatocyte Functionality for Liver Toxicity Screening

Sreenivasa C. Ramaiahgari, Suramya Waidyanatha, Darlene Dixon, Michael J. DeVito, Richard S. Paules, and Stephen S. Ferguson[1]

Division of the National Toxicology Program, National Institute of Environmental Health Sciences, NIH, Durham, North Carolina 27709

[1]To whom correspondence should be addressed at Biomolecular Screening Branch, Division of the National Toxicology Program, National Institute of Environmental Health Sciences, Mail Code K2-17, P.O. Box 12233, Research Triangle Park, Durham, NC 27709. Fax: 919-541-1019. E-mail: stephen.ferguson@nih.gov.

ABSTRACT

Effective prediction of human responses to chemical and drug exposure is of critical importance in environmental toxicology research and drug development. While significant progress has been made to address this challenge using *in vitro* liver models, these approaches often fail due to inadequate tissue model functionality. Herein, we describe the development, optimization, and characterization of a novel three-dimensional (3D) spheroid model using differentiated HepaRG cells that achieve and maintain physiologically relevant levels of xenobiotic metabolism (CYP1A2, CYP2B6, and CYP3A4/5). This *in vitro* model maintains a stable phenotype over multiple weeks in both 96- and 384-well formats, supports highly reproducible tissue-like architectures and models pharmacologically- and environmentally important hepatic receptor pathways (ie AhR, CAR, and PXR) analogous to primary human hepatocyte cultures. HepaRG spheroid cultures use 50–100× fewer cells than conventional two dimensional cultures, and enable the identification of metabolically activated toxicants. Spheroid size, time in culture and culture media composition were important factors affecting basal levels of xenobiotic metabolism and liver enzyme inducibility with activators of hepatic receptors AhR, CAR and PXR. Repeated exposure studies showed higher sensitivity than traditional 2D cultures in identifying compounds that cause liver injury and metabolism-dependent toxicity. This platform combines the well-documented impact of 3D culture configuration for improved tissue functionality and longevity with the requisite throughput and repeatability needed for year-over-year toxicology screening.

Key words: 3D; spheroids; xenobiotic metabolism; *in vitro*; HepaRG; nuclear receptor.

INTRODUCTION

The liver is the principal organ for chemical metabolism in humans. To model liver and chemical-induced effects on hepatic molecular pathways, it is essential to develop *in vitro* liver models that possess tissue-like functionality. Primary human hepatocytes (PHHs) are the "gold standard" first choice for predicting drug metabolism and liver enzyme induction in humans, and have begun to emerge in importance for toxicology research. However, their finite supply, high degree of inter-donor variability, and limited longevity present significant challenges to model a broader complement of toxicological response to chemical exposure. Immortalized cell lines offer alternatives to PHHs (ie HepG2, Fa2N-4, HuH-7 and Hep3B) and are widely used in screening assays, but they possess extremely low or

undetectable levels of major drug/xenobiotic metabolism enzymes, and a high degree of karyotype abnormalities (Guo *et al.*, 2011; Wong *et al.*, 2000). Recent technological advances with "next-generation" *in vitro* models employing micro-patterning, extracellular gel matrices, bio-printing, bioreactors, spheroid generation, microfluidic flow models, and others approaches have improved longevity and differentiation states with PHHs and immortalized cell lines (Darnell *et al.*, 2011; Gunness *et al.*, 2013; Khetani *et al.*, 2013; Leite *et al.*, 2012; Mueller *et al.*, 2014; Nguyen *et al.*, 2016; Novik *et al.*, 2010; Ramaiahgari *et al.*, 2014). However, most of these approaches, while promising, currently lack necessary throughput to assess concentration-response (and time), or simplicity in design (ie laborious steps, increased variation, decreased success rates, gels/matrices that nonspecifically bind compounds) for predictive toxicology/pharmacology screening.

HepaRG cells derived from human hepatocellular carcinoma have emerged as a promising alternative to PHHs. These bipotent progenitor cells are expanded and differentiated over approximately 4 weeks into "differentiated" co-cultures of hepatocyte- and cholangiocyte-like cells in 2D culture configurations, (Aninat *et al.*, 2006; Gripon *et al.*, 2002; Guillouzo *et al.*, 2007). Recent efforts to cryopreserve "fully" differentiated HepaRG cells have enabled global accessibility that, under appropriate culture conditions (ie differentiation medium), recover and maintain drug metabolism activity and hepatocyte functionality (Jackson *et al.*, 2016; Mueller *et al.*, 2014). It is the combination cell "type" and cell culture configuration (ie cell–cell and cell–matrix interactions) (Yamada and Cukierman, 2007) that dictates the fidelity and functionality of *in vitro* liver models. Ideally, cell types applied in compound screening should have year-over-year availability with a consistent genetic background, support a stable highly differentiated tissue-like functionality in multi-well formats (ie 96- and 384-well), and possess tissue-like responsiveness to compound exposures over multiple weeks. In recent years, several three-dimensional (3D) HepaRG models have been reported to better mimic *in vivo*-like microenvironments. These models show improved hepatocyte differentiation, longevity, and functionality compared with 2D HepaRG cultures (Darnell *et al.*, 2012; Gunness *et al.*, 2013; Leite *et al.*, 2012). However, to date, these 3D HepaRG models lack sufficient simplicity in design, capacity for medium-throughput compound screening, characterization of xenobiotic metabolism competence compared with the "gold standard" of PHH suspensions, and characterization of hepatocyte functionality.

Herein, we describe the development of 96- and 384-well 3D spheroid cultures of HepaRG cells in ultra-low attachment plates which support spheroidal differentiation in a simple one-step process. We optimized cell culture conditions to produce uniform spheroid-like structures and maintain a stable spheroid phenotype with high levels of CYP450 enzyme activity for up to 28 days. These spheroids exhibit several hallmarks of polarized hepatocyte architecture and functionality. Pharmacologically important cytochromes P450 enzymatic activities (CYP1A2, CYP2B6, and CYP3A4/5) were observed to far-exceed (approximately 10×) levels in sandwich cultures of PHHs (SC-PHHs) achieving near-median activities observed across hundreds of donor preparations of PHH suspensions immediately removed/cryopreserved from human liver tissue. Prototypical activators of AhR, CAR and PXR hepatic receptors showed liver enzyme induction of associated cytochrome P450 enzymes consistent with a highly functional *in vitro* liver model mirroring human liver response to compound exposures. Compounds that require metabolic activations such as aflatoxin B1 showed concentration-related cytotoxicity which was attenuated by Inhibition of P450 activities, highlighting the potential for this system to model metabolism-dependent toxicity. The stable long-term phenotype of spheroids (>28 days) offers feasibility for longer term repeated exposure studies. Indeed, repeated exposures on HepaRG spheroids showed increased sensitivity in identifying compounds that have potential for drug induced liver injury (DILI). This novel platform for toxicology screening combines physiologically relevant levels of xenobiotic metabolism with a high degree of tissue-like architecture, hepatocyte functionality, and sufficient throughput to study concentration and time-dependent relationships.

MATERIALS AND METHODS

HepaRG cell culture. For 3D spheroid cultures, cryopreserved differentiated HepaRG cells (Triangle Research Labs, Durham NC which was recently acquired by Lonza, Walkersville, MD) were thawed and seeded at 1000 cells per well onto round bottom ultra-low attachment (ULA) plates, (Corning Inc, catalog: 4520 (96-well) or 3830 (384-well), New York, NY) in 50 μl Williams E medium (ThermoFisher, Waltham, MA) supplemented with induction additive MHPIT (Triangle Research labs, Durham NC). Initially, seeding density was optimized by adding cell densities between 1000 and 20 000 cells to the plate and analyzing for CYP1A2, CYP2B6, and CYP3A4/5 activities and spheroid morphology. One thousand cells per well in 96/384-well plates showed optimal P450 enzymatic activities and morphologies, which were subsequently used for the entire study. Culture media were refreshed every 2–3 days by removing 30 μl (from 50 μl total medium per well) and adding fresh 30 μl medium using Viaflo semi-automated liquid handler (Integra Biosciences, Hudson, NH), and spheroids were maintained for up to 28 days in culture. All the assays, with exception of immunohistochemical analysis (Figure 1A), were performed in 384-well plates, both 96/384 well showed similar morphology and we anticipate no morphological and physiological changes with plate formats. For 2D monolayer cultures, 100 000 (96-well) or 25 000 (384-well) cells were seeded per well in collagen-coated plates in Williams E medium supplemented with MHTAP plating additive (Triangle Research labs, Durham, NC). After 24 h, media were changed to induction medium MHPIT as above. PHHs were cultured with a seeding density of 20 000 cells per well on collagen-coated 384-well plates. Four-hour post-seeding, media were exchanged and cells were overlaid with 0.35 mg/ml of Matrigel (Corning, New York, NY) in maintenance medium comprised of Williams E medium supplemented with 15 mM HEPES (ThermoFisher, Waltham, MA), 1× ITS+ (Corning, New York, NY), 1× Glutamax (ThermoFisher, Waltham, MA), 100 nM dexamethasone and 25 U/ml penicillin and 25 μg/ml streptomycin.

HepaRG spheroid size assessment. HepaRG spheroids cultured for 21 days were stained with nuclei dye Hoechst 33342 (ThermoFisher, Waltham, MA) suitable for live cell imaging assays. Briefly, 10 ng/ml of Hoechst 33342 was prepared in cell culture medium and added to the spheroids. After 15-min incubation, spheroids were imaged for nuclei and cellular morphology by phase contrast imaging taking 20 Z-sections of each spheroid using a high content imager, ImageXpress micro (Molecular Devices, Sunnyvale, CA). A "maximum intensity projection image" of the spheroid was generated from 20 Z-sections imaged in the nuclei channel from 384-well plates. This "maximum intensity projection image" was analyzed with multi-wavelength cell scoring settings on Metaxpress image

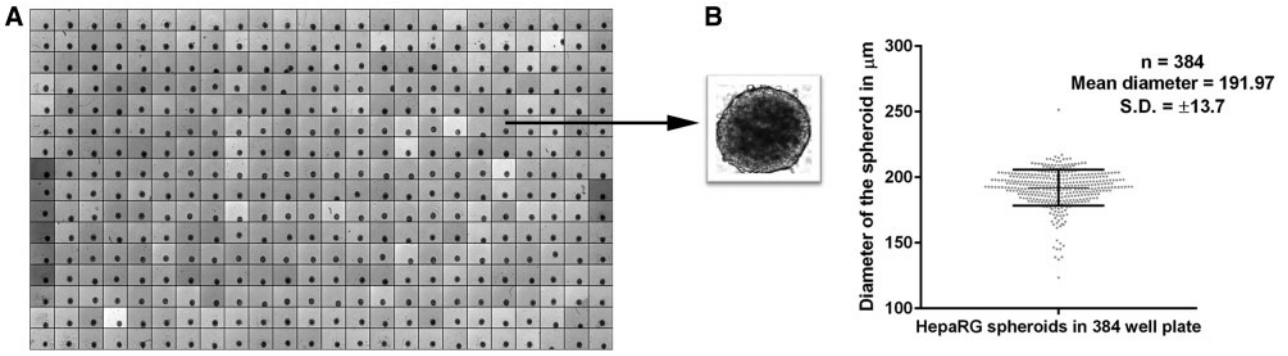

Figure 1. Morphology of HepaRG spheroids. HepaRG cells seeded at 1000 cells per well form spheroids-like structures. Single spheroid per well in a 384-well plate (A); size of the spheroid is approximately 191.97 μm (B).

analysis software (Molecular Devices, Sunnyvale, CA). The analysis provides numerical value for area of the spheroid. Diameter was calculated from the area, mean diameter, and SD of these 384 spheroids was plotted in Figure 2.

Immunohistochemical and immunofluorescent staining. For immunohistochemical staining, HepaRG spheroids were collected from ULA plates into Eppendorf tubes containing 4% formaldehyde, fixation was performed for 10 min and spheroid suspension was spun at 1000 rpm for 2 min. The resulting pellet was washed with phosphate buffered saline (PBS) and embedded in paraffin. Tissue sections of 3 μm were prepared and stained with hematoxylin/eosin, PAS (Periodic acid-Schiff's reaction) and PAS after treatment with diastase to remove glycogen. Immunohistochemical detection of multidrug resistance-associated protein MRP2 (Abcam, Cambridge, MA; catalog: ab3373), cytokeratin CK19 (Millipore, Temecula, CA; catalog: MAB3238), cytochrome P450 enzyme CYP3A4 (Abcam, Cambridge, MA; catalog: ab135813) and canalicular protein carcinoembryonic antigen CEA (Dako, Agilent Pathology Solutions, Santa Clara, CA; catalog: A0115) was performed. Immunofluorescent staining was performed on 21-day-old spheroids for MRP2 (Abcam, Cambridge, MA; catalog: ab3373). Here, spheroids were collected in Eppendorf tubes, and fixation was performed as described earlier. Spheroids were washed twice with PBS and permeabilized with 0.2% of Triton-X for 10 min followed by blocking with 1% BSA in PBST (PBS with 0.2% Tritox-X). Spheroids were then incubated with anti-MRP2 antibody (1:250 dilution in 1% BSA-PBST) overnight at 4 °C. After incubation, spheroids were washed 3 times with PBS and incubated with secondary antibody Alexa 488 goat anti-mouse IgG (A11029, ThermoFisher, Waltham, MA) for 1 h followed by counter staining with Hoechst 33358 (Enzolife Sciences, Farmingdale, NY). Confocal images were acquired on Zeiss LSM 780 (Zeiss, Oberkochen, Germany).

P450 enzymatic activity assays. HepaRG cells in 2D and 3D configurations were assessed for xenobiotic metabolism competence with *in situ* metabolism assays using the probe substrates bupropion (CYP2B6, 500 μM), phenacetin (CYP1A2, 400 μM) and midazolam (CYP3A4, 10 μM) as previously described (Jackson *et al.*, 2016). Supernatants were collected after 60-min incubations and stored at −80 °C for analysis by LC/MS-MS. Analyses were performed with an API 5000 triple quadrupole mass spectrometer (SCIEX, Concord, Ontario, Canada). The analytical method used was a modification of protocol described earlier (Walsky and Obach, 2004). Briefly, 50 μl of incubation medium samples from each well were transferred to a 96-well plate and 170 μl of 0.1% formic acid in acetonitrile was added along with 10 μl of isotopically labeled internal standard mixture (250 ng each per milliliter in acetonitrile). Samples were mixed, centrifuged (4000 rpm for 5 min) and 100 μl of the supernatant was transferred to a Waters Acquity 96-well plate and mixed with 100 μl of methanol: water (1:1). Standard curves ranged from 1 to 1000 ng/ml. Standards were prepared by mixing 50 μl of blank medium with 10 μl of spiking solution of each compound and extracting the same to the samples. Accuracy of all standards were within 15% of nominal for all concentrations except at LOQ (1 ng/ml) where it was within 20% of nominal. Standard curves were fit using a quadratic equation with 1/× weighting. Concentration of samples were calculated by using the analyte peak area/internal standard peak area and using regression analysis in Analyst 1.6.2 (SCIEX, Concord, Ontario, Canada) to determine the ng/ml quantities. A complete list of instrumentation and analysis parameters are described in Supplementary data 1. Historical cytochromes P450 enzymatic activity data with PHH suspensions and sandwich cultures across numerous donor preparations were described previously (Jackson *et al.*, 2016).

Assessment of hepatobiliary transport in HepaRG cells. A synthetic fluorescent bile acid analog, cholyl-lysyl-fluorescein, CLF (Corning, New York, NY) with similar biological activity as cholyl glycine, was used to determine the hepatobiliary transport activity. HepaRG spheroids were rinsed with 1× Hanks balanced salt solution (ThermoFisher, Waltham, MA) and incubated with 5 μM CLF and 10 ng/ml of Hoechst 33342 in HBSS for 15 min. After the incubation period, the cells were washed 3 times with HBSS and imaged live on Zeiss LSM 780 (Zeiss, Oberkochen, Germany). A series of images were collected across the Z-plane of the spheroid, and a maximum intensity projection image was generated using the image processing software package, Image J (https://imagej.nih.gov/ij/; last accessed June 21, 2017).

P450 induction assays. HepaRG spheroids were cultured for 10 days in 384-ULA plates. Spheroids were then incubated with 3.16-fold dilutions of omeprazole, phenobarbital, rifampicin and CITCO with concentrations starting at 100, 3160, 3.16, and 10 μM, respectively. Williams E medium supplemented with 15 mM HEPES, 1× ITS+, 1× Glutamax, 100 nM dexamethasone and 25 U/ml penicillin and 25 μg/ml streptomycin was used in spheroid cultures for liver enzyme induction assays. Media with fresh compounds were changed every 24 h over a 72-h treatment period. After 72 h of exposure, eight spheroids were pooled together and lysed with Qiazol reagent (Qiagen, Germantown, MD) and RNA was extracted

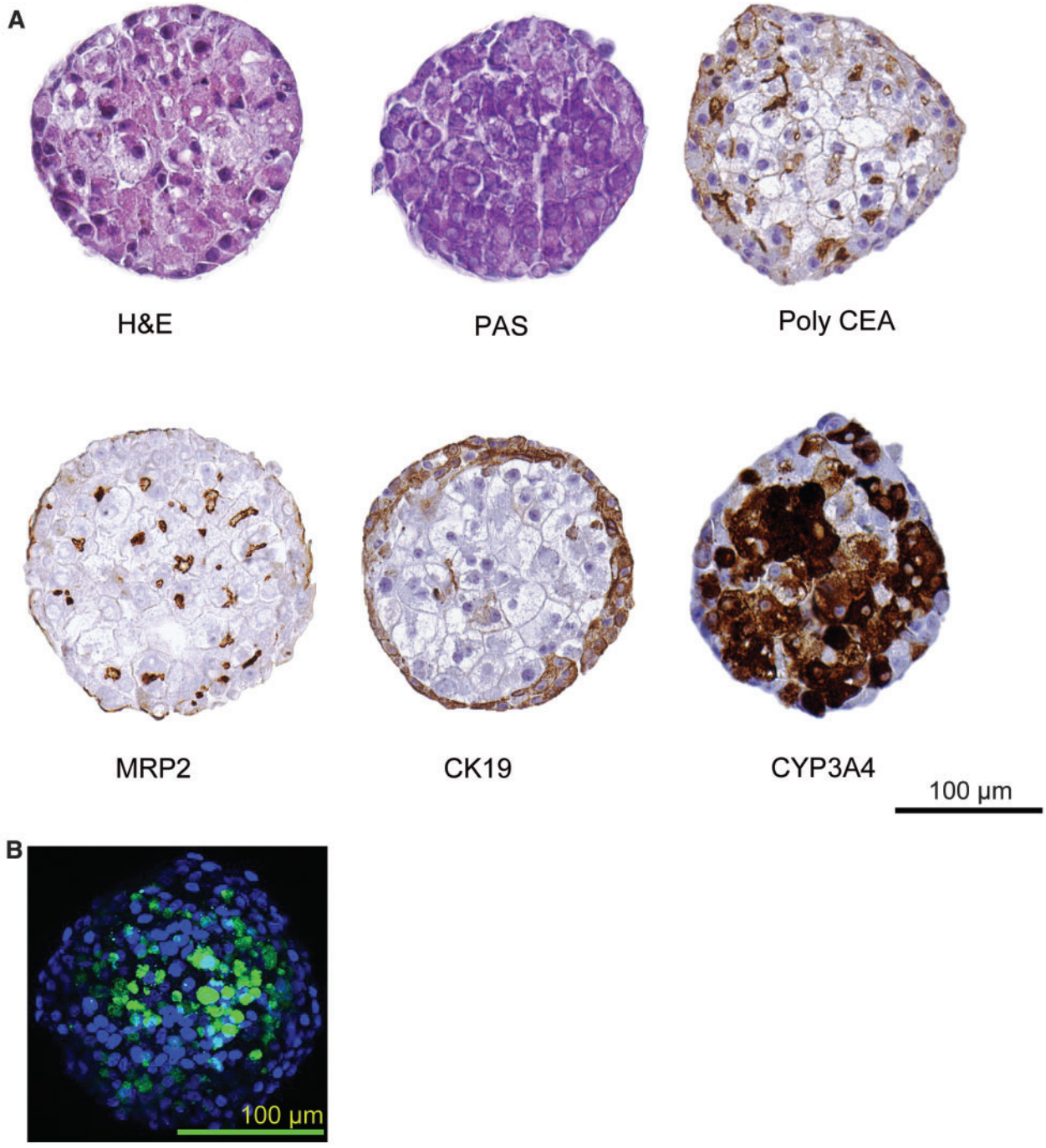

Figure 2. Immunohistochemical analysis of HepaRG spheroids. HepaRG spheroids stained for H&E (haematoxylin and eosin) stain, PAS (periodic Schiff's), Poly CEA (carcinoembryonic antigen), MRP2 transporter, cytokeratin 19 and CYP3A4 (Scale bar 100 µm). Merged image of synthetic bile acid analogue, cholyl-lysyl-fluorescein (CLF) (green) and nuclei (blue) in HepaRG spheroid (Scale bar 100 µm).

as per manufacturer's protocol. High-Capacity cDNA Reverse Transcription Kit (ThermoFisher, Waltham, MA) was used for cDNA synthesis using 200 ng of RNA from each sample. Real time PCR analysis was performed using TaqMan probes and TaqMan Universal PCR master mix (ThermoFisher, Waltham, MA) with Quantstudio 7 real-time PCR system (ThermoFisher, Waltham, MA) according to the manufacturer's protocol. Briefly, a 10-µl reaction mixture was prepared using 1 µl of cDNA, 5 µl of PCR mix and 4 µl of water. Real-time PCR cycles were 95 °C for 10 min, followed by 40 cycles of 95 °C (20 s), 60 °C (60 s). TaqMan assay probes (ThermoFisher, Waltham, MA) used are Hs04183483_g1 (CYP2B6), Hs00604506_m1 (CYP3A4), Hs02758991_g1 (GAPDH), Hs00167927_m1 (CYP1A2). mRNA levels of target genes were normalized to housekeeping gene GAPDH. Data are expressed as fold-change to vehicle control.

Metabolically activated cytotoxicity with aflatoxin B1 and modulation with P450 inhibitor. HepaRG spheroids (384-well) were exposed to aflatoxin B1 (Sigma–Aldrich, St. Louis, MO) in concentration-response at a top concentration of 10 µM with 1.5-fold serial

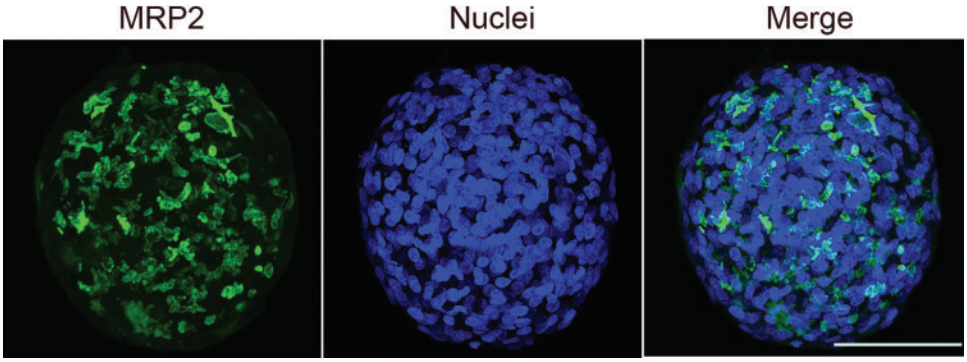

Figure 3. MRP2 localization in HepaRG spheroids. Immunofluorescent staining of MRP2 (green) and nuclei (blue) on HepaRG spheroids (scale bar 100 μm).

dilutions down to 200 nM in the presence or absence of pan-P450 inhibitor 1-aminobenzotriazole (ABT, 1 mM), (Sigma–Aldrich, St. Louis, MO). Cell viability was assayed using the CellTiter-Glo (Promega, Madison, WI) assay system to monitor relative levels of ATP by luminescence using the manufacturer's protocol. Luminescence was measured on a CLARIOstar (BMG LABTECH, Ortenberg, Germany).

Assessment of cytotoxicity. Primary human hepatocytes (Donor: HU8192, Male, ThermoFisher, Waltham, MA) were cultured for 24 h in 384-well plates prior to compound exposures. HepaRG cells in 2D confluent monolayer cultures (20 000 cells per well) and 3D spheroids (1000 cells per well) were cultured for 21 days. Repeated dosing on HepaRG spheroid cultures was performed between day 21 and day 28 (three doses were administered at day 22, 24, and 26) and cell viabilities were assessed on day 28. All the compounds were obtained from Sigma–Aldrich, St. Louis, MO; concentrations used were shown in Supplementary Table 5. CellTiter-Glo reagent (Promega, Madison, WI) was used for analyzing cell viability upon compound exposure following the manufacturer's protocol. Luminescence signal was measured on a Clariostar (BMG Labtech, Ortenberg, Germany) plate reader. Luminescence signal was directly proportional to total amount of ATP present in the cells, which was measured as an indicator of cellular stress/cytotoxicity.

Statistical analysis. Data were normalized and expressed as the mean ± SD of three independent experiments, unless otherwise stated, using Microsoft Excel. Graphs were plotted using GraphPad Prism 7 (GraphPad software, San Diego, CA). Significance levels were calculated using GraphPad Prism software by performing either an unpaired Student's *t*-test or in case of multiple comparisons a 2-way analysis of variance (ANOVA) where, $^{*}P < 0.05$, $^{**}P < 0.01$, $^{***}P < 0.0001$.

RESULTS

HepaRG Cells Form Spheroids in 96/384-Well ULA Plates

HepaRG cells, seeded at a density of 1000 cells per well, in 96/384-well ULA plate, self-aggregated to form spheroid-like structures without addition of exogenous ECM components. From Days 1–3, individual cells appeared to aggregate while reaching compact spherical units by Day 7 in culture. The diameter of spheroids across a 384-well plate (Figure 1A) was measured to be 192 ±14 μm (Figure 2A). The shape and size of the spheroids was largely unchanged after Day 7 out to 28 days (cultures were terminated, but likely viable for much longer). Optimization of initial cell seeding densities revealed 1000 cells per well to be ideal for generating organized spherical structure with higher levels of drug metabolism enzyme activities. Cell numbers greater than 2000 cells per well, formed aggregates, but displayed delayed or aberrant formation of spherically compact structures with lower drug metabolizing enzyme activities (Supplementary Figure 2B). This could be due to the formation of necrotic cores in the center of spheroids with increasing size as observed in the earlier studies where spheroids above 250 microns lead to hypoxia and necrotic cores (Asthana and Kisaalita, 2012). Taken together, these results demonstrate that HepaRG cells effectively and reproducibly form 3D microtissues in 384-well ULA plates in a simple one-step process and highlights the importance of initial cell seeding densities on spheroidal architectures and xenobiotic metabolism competence.

HepaRG Spheroid Differentiation Leads to Tissue-Like Architectures With Polarized Organization and Function

Hepatocyte cellular polarity and differentiation are lost when cells are removed from their native *in vivo* tissue (Levine and Stockdale, 1985). H&E staining was used to study cellular organization and morphological features associated with health and physiological functions of the spheroids. HepaRG spheroids showed well-organized nuclei and cytoplasm without signs of necrotic or apoptotic centers.

In vivo, the apical surface of adjacent hepatocytes form a lumen called "bile canaliculi" into which bile is secreted from hepatocytes. Hepatocytes are arranged in chords and lumen from adjacent hepatocytes form bile canalicular networks that transport bile to bile ducts (Treyer and Musch, 2013). To visualize the extent of modeling these features in HepaRG spheroids, we stained for multidrug resistance protein 2 (MRP2), a bile canalicular efflux transporter involved in drug and bile salt/acid transport (Kullak-Ublick *et al.*, 2002). MRP2 staining revealed extensive networks of canalicular domains at the apical surface of HepaRG spheroids (Figs. 2 and 3; Supplementary Movie 3). This observation was further substantiated by the presence of poly CEA staining in the luminal regions of the spheroids (Figure 2); poly CEA binds to glycoprotein-1 on canalicular surfaces. We later investigated the bile acid transport activity in HepaRG spheroids by using a synthetic bile acid analogue, cholyl-lysyl-fluorescein (CLF). CLF is taken up by the organic anion-transporting polypeptide OATP1B3 present at the basal surface of hepatocytes and is then excreted into bile canaliculi via MRP2 (de Waart *et al.*, 2010). CLF was found to be localized in the bile

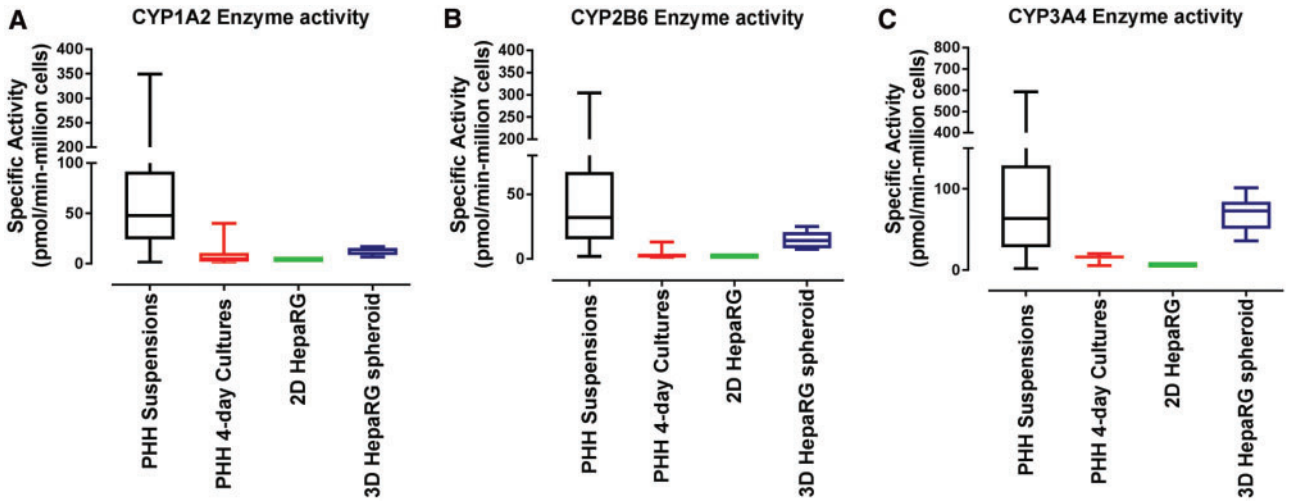

Figure 4. CYP450 enzyme activity in 2D HepaRG cells, HepaRG spheroids and primary human hepatocytes. LC-MS/MS analysis of metabolite formation rate of acetaminophen (CYP1A2); 1-hydroxybupropion (CYP2B6) and 1-hydroxymidazolam (CYP3A4). Data were the mean of three independent experiments (± SEM) from 10-day sandwich-cultured 2D HepaRG cells and 21-day cultured 3D HepaRG spheroids. Data from primary suspension cultures were from 212, 137 and 132 individual donor preparations for CYP1A2, CYP2B6 and CY3A4/5, respectively, and 52 individual donor preparations for 4-day sandwich–cultured primary hepatocytes.

canalicular regions at the luminal surface of the spheroids (Figure 2B). The tissue-like presence of MRP2, CEA staining, and live-cell localization of CLF demonstrating functional bile acid transport activity clearly demonstrates the formation of bile-canaliculi-like structures and a polarized architecture with 3D HepaRG spheroids analogous to hepatocytes *in vivo*.

Cryopreserved HepaRG cells are commercially provided in a differentiated/cryopreserved form containing both hepatocyte- and cholangiocyte-like cells (Jackson *et al.*, 2016). HepaRG cells stained with the cholangiocyte marker CK19 (Day 7 in culture) appear somewhat localized at periphery of HepaRG spheroids (data not shown), and becomes more pronounced by Day 21 in culture and predominantly localized at the "basal" surface of the spheroid (Figure 2). A similar type of cholangiocyte arrangement at the periphery of the spheroids was recently reported with PHH co-cultures with nonparenchymal cells (Bell *et al.*, 2016) suggesting this type of organization is not selective to HepaRG spheroids.

An important function of hepatocytes in liver is the storage of glycogen that helps in energy metabolism. Therefore, we characterized the glycogen storage functionality of 3D HepaRG spheroids with the periodic acid-Schiff (PAS) stain (Figure 2). PAS staining revealed extensive staining within HepaRG spheroids consistent with a robust capacity for glycogen storage.

Finally, a hallmark of hepatocyte functionality is the capacity for drug metabolism. CYP3A4 is known as one of the most pharmacologically important cytochrome P450 enzymes in human liver (Zanger and Schwab, 2013), We observed pronounced expression of CYP3A4 protein that appeared to be enriched in the interior of spheroids (Figure 2). These data are consistent with a high degree of metabolic competence and support the results with CK19 staining which show hepatocyte-like cells localized within the interior of HepaRG spheroids while cholangiocyte-like cells appear predominantly across the periphery. Taken together, these 3D HepaRG imaging data indicate tissue-like architectures and functionality, and some unique features specific to these spheroidal configurations of HepaRG cells consistent with emerging co-culture models of human liver.

HepaRG Spheroids Exhibit Physiologically Relevant Levels of Drug Metabolism Activity

Physiological-relevant xenobiotic metabolism functionality is essential for predicting human drug metabolism and metabolite-associated toxicities. Near-physiological levels of xenobiotic metabolism enzymes are present in suspensions of PHHs directly derived from human liver and immediately used (or cryopreserved), and represent the "gold standard" of metabolic competence for human drug metabolism prediction. However, these suspensions of PHHs are short lived (a few hours) and de-differentiate when cultured in conventional 2D configurations losing approximately 90% of their initial metabolic competence (Smith *et al.*, 2012) within the initial 1–2 days in culture. Therefore, we assessed the drug metabolism competence of HepaRG cells in 2D and 3D spheroid configurations in context with suspensions and sandwich cultures of PHHs. Specific activities of three major P450 enzymes (CYP1A2, CYP2B6 and CYP3A4) important in human drug metabolism were analyzed. CYP1A2 activity, measured by acetaminophen formation rates from phenacetin metabolism were 12.9 ± 3.98 pmol/min-million cells (Day 21, $n = 3$) with HepaRG spheroids, whereas 2D HepaRG cultures produced 4.27 ± 0.459 pmol/min-million cells ($n = 3$) (Figure 4A). In context, CYP1A2 activity across 52 donor preparations of sandwich cultured PHHs ranged from 0.072 to 40 pmol/min-million cells with a median of 4.94 pmol/min-million cells and 25th percentile of 1.89 pmol/min-million cells. Suspension of PHHs representing P450 activities approximating human liver tissue ranged from 1 to 349 pmol/min-million cells (212 donor preparations) with a median of 48 pmol/min-million cells and 25th percentile of 24.2 pmol/min-million cells (Figure 4A). These data confirm that HepaRG spheroids produce physiologically relevant levels of CYP1A2 enzymatic activities that approach the 25th percentile of PHH suspensions (within 2-fold), far-exceed (>7-fold) levels in sandwich cultures PHHs, and offer a key advantage over conventional 2D culture methods of HepaRG cells previously observed to intrinsically produce proportionally lower levels of CYP1A2 activity compared with CYP2B6 and CYP3A4/5 activity levels (Jackson *et al.*, 2016).

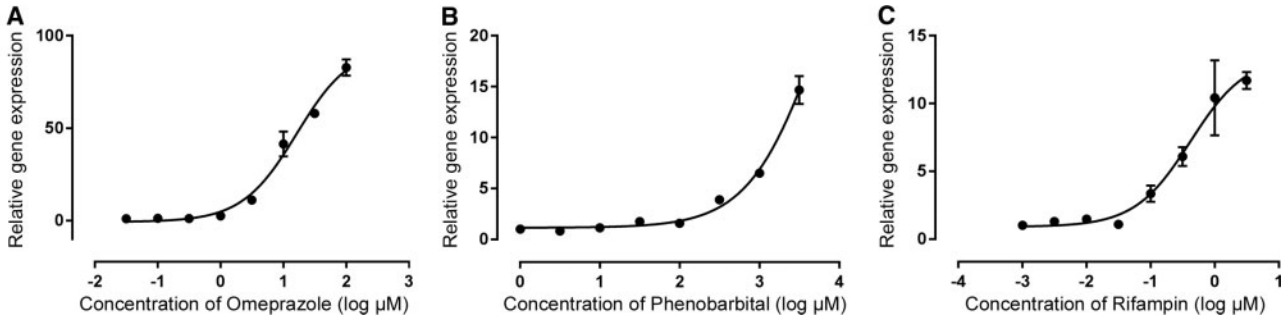

Figure 5. AhR, CAR, PXR induction assay. HepaRG spheroid cultures were treated with Prototypical inducers if AhR (Omeprazole); CAR (Phenobarbital) and PXR (Rifampin) for 72 h with fresh addition of compound every 24 h. Data were normalized to GAPDH, representative of two independent experiments (± SD).

CYP2B6, another pharmacologically important enzyme, is highly inducible in response to nuclear receptor activation (CAR & PXR) in human liver and SC-PHH. HepaRG spheroids produced high constitutive levels of CYP2B6 activity (formation rates of 1-hydroxybupropion from bupropion) compared with 2D HepaRG cultures (14.8 ± 7.08 pmol/min-million cells vs 1.93 ± 0.0754 pmol/min-million cells) (Figure 4B). CYP2B6 activity across 52 donor preparations of sandwich-cultured PHHs ranged from 0.210 to 13.1 pmol/min-million cells with a median of 2.16 pmol/min-million cells and 25th percentile of 1.06 pmol/min-million cells, while suspensions of PHHs (137 donor preparations) ranged from 1.86 to 304 pmol/min-million cells with a median of 32.1 pmol/min-million cells and 25th percentile of 15.3 pmol/min-million cells. These data demonstrate that 3D HepaRG spheroids support liver-like CYP2B6 enzymatic activities superior to 2D cultures of HepaRG or PHHs, and achieve comparable levels to the 25th percentile of PHH suspensions (14.7 vs 15.3 pmol/min-million cells) (Figure 4B).

Similarly, CYP3A4/5 activity, measured by formation rates of 1-hydroxymidazolam from midazolam with 3D HepaRG spheroids, far-exceeded 2D HepaRG activity levels (69.4 ± 21.1 pmol/min-million cells vs 6.67 ± 0.392 pmol/min-million cell) (Figure 4C). In context, PHH sandwich cultures ranged from 5.5 to 20.1 pmol/min-million cells, while PHH suspensions (132 donor preparations) ranged from 1.54 to 593 pmol/min-million with a median of 63.7 pmol/min-million cells and 25th percentile of 28.6 pmol/min-million cells (Figure 4C). These data are consistent with the trends observed with CYP2B6 enzymatic activity demonstrating robust levels of CYP3A4/5 enzymatic activity from 3D HepaRG spheroids that are comparable to median PHH suspension levels (69.4 vs 63.7), far exceed 2D HepaRG and PHHs (approximately 10-fold), and do not require high concentrations of DMSO to maintain a high degree of metabolic competence.

Recently, sandwich culture configurations have been suggested as an alternative to high concentrations of DMSO to improve the metabolic competence with HepaRG cells (Aninat *et al.*, 2006; Jackson *et al.*, 2016). Therefore, we compared the CYP1A2, CYP2B6, and CYP3A4/5 enzymatic activities of HepaRG cells in 2D cultures with and without extracellular matrix (ECM) overlay using various commercially available HepaRG media supplement types and overlay start times compared with 3D HepaRG spheroids (Supplementary Figure 2A). Spheroids of HepaRG cells showed significantly higher activities (>2.6- to 5.8-fold, $P < 0.0001$) than all 2D culture conditions. It is notable that the time-dependent "rebound" of enzymatic activity with 2D cultures over the course of 10 days was dependent on the commercial source of HepaRG supplementation. It is also important to note that HepaRG cells optimally formed well-defined spheroid-like structures with induction and plating media, while other supplements recommended for metabolism studies or plating the cells supported more asymmetrical aggregate-like HepaRG cultures in the 96- and 384-well ULA plates. Unlike PHH cultures, HepaRG spheroids are capable of stably maintaining a high degree of metabolic competence for multiple weeks in 2D configurations compared with approximately 1 week with PHHs (Supplementary Figure 2C). This advantage is critical for studying slower-developing chemical–biological interactions and their quantitative translation to humans.

Hepatic Nuclear Receptor Functionality and Liver Enzyme Induction With 3D HepaRG Spheroids

A hallmark of highly differentiated hepatocyte functionality in human liver tissue is the ability to respond to xenobiotic activation of key receptor signaling pathways that include signaling through the pregnane X receptor (PXR), constitutive androstane receptor (CAR), and aryl-hydrocarbon receptor (AhR) to induce liver enzyme expression in humans (Levy *et al.*, 2015). It is also known that chronic activation of these hepatic receptors in rodents can lead to liver tumor formation (Elcombe *et al.*, 2014; Parkinson, 1996). Finally, it is conceivable that the higher levels of drug metabolizing activity in HepaRG spheroids simply represents an induced, "Zone 3"-like metabolic competence akin to 2D HepaRG under high DMSO concentrations. Therefore, we investigated the functionality of 3D HepaRG spheroids to respond to clinically relevant activators of AhR, CAR, and PXR hepatic receptor pathways to induce expression of sentinel gene targets CYP1A2, CYP2B6 and CYP3A4, respectively. These pathways are effectively modeled with SC-PHHs to predict clinical outcomes for liver enzyme induction in humans and are required by US FDA during drug development (Chu *et al.*, 2009). Inducers omeprazole (AhR), phenobarbital (CAR), and rifampicin (PXR) were evaluated with 3D HepaRG spheroids in concentration-response as shown in Figure 5. Here, CYP1A2 mRNA content was effectively induced with omeprazole, reaching maximal inducibility of 82.8-fold-over-control with 100 μM (EC_{50} value of 16 μM) (Figure 5A). Similarly, a 11.7-fold increase in CYP3A4 mRNA content was observed with 3.16 μM rifampicin with an EC_{50} of 0.41 μM (Figure 5B), which was within the ranges observed with SC-PHH cultures (Hariparsad *et al.*, 2008; Zhang *et al.*, 2014) and a 14.6-fold CYP2B6 induction mRNA content with phenobarbital treatment up to 3.16 mM (Figure 5C). We have also evaluated CYP2B6 induction using a direct CAR activator CITCO (Supplementary Figure 4), and observed a concentration-related induction of approximately 9-fold with an EC_{50} of 25.8 nM. Collectively, these data demonstrate 384-well HepaRG spheroid cultures effectively model hallmark pathways AhR, CAR, and PXR analogous to PHH cultures while maintaining basal metabolic competence. Taken together, the drug

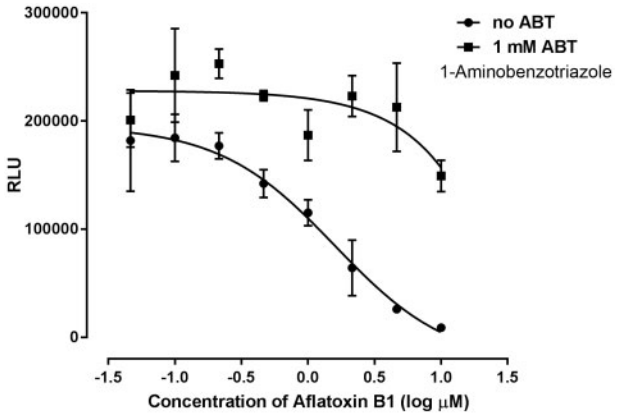

Figure 6. Metabolism dependent toxicity in HepaRG spheroids. HepaRG spheroid cultures at day 21 were treated with aflatoxin B1 in the presence and absence of 1 mM 1-Aminobenzotriazole (1-ABT) and cell viability was assessed after 24 h. Data are the means of three independent experiments ± SD.

metabolism competence, proficiency to transport CLF into biliary compartments, evidence of tissue-like cellular architectures, and functional hepatic receptor signaling pathways demonstrates the high degree of tissue-like differentiation and functionality with these 3D HepaRG spheroids.

HepaRG Spheroids Model Metabolically Activated Cytotoxicity

Many chemicals are either detoxified or converted into toxic metabolites by xenobiotic metabolizing enzymes. As HepaRG spheroids exhibited physiologically relevant levels of pharmacologically important drug metabolizing activity, we investigated the utility of this model to identify metabolism-dependent impacts on cell viability. For this, we assessed the impact of a well-studied mycotoxin aflatoxin B1 known to be metabolized by CYP3A4 and CYP1A2 to form a toxic metabolite (AFB1-8,9-exo-epoxide) that binds to DNA and can result in mutations (Gallagher *et al.*, 1996; Wild and Turner, 2002). Here, HepaRG spheroids treated with aflatoxin B1 showed a concentration-dependent cytotoxicity with TC_{50} of 1.6 μM (Figure 6). This metabolism-driven cytotoxicity was observed at a higher potency (lower TC_{50}) in HepaRG spheroids (TC_{50} of approximately 1 μM) compared with an earlier study with PHHs with TC_{50}=37.6 μM; HepG2 with TC_{50}=240.5 μM and stem cell-derived hepatocytes with TC_{50} ranging from 81.4 to 143.7 μM (Kang *et al.*, 2016). These results are consistent with the improved liver-like CYP3A metabolism observed with 3D HepaRG spheroids. To confirm a role for xenobiotic metabolism in the observed aflatoxin B1 cytotoxicity, treatment with 1-ABT (1 mM), a nonspecific irreversible pan-P450 inhibitor (Linder *et al.*, 2009) was evaluated (Figure 6). The presence of ABT caused a marked attenuation of aflatoxin B1 cytotoxicity that was consistent with a P450-activated cytotoxicity. These data, combined with the observed liver-like levels of xenobiotic metabolism competence, demonstrate that 3D HepaRG spheroids have potential to effectively model and screen compounds for potential metabolically activated toxicity.

Chemical Induced Liver Injury Modeling With HepaRG Spheroids

Liver toxicity remains a principle cause of drug attrition during pharmaceutical drug development (Ostapowicz *et al.*, 2002). Despite significant advances with *in vitro* liver models for predicting human drug metabolism, there are limitations associated with existing approaches due to limited longevity of cells/cultures and reduced differentiation (ie metabolic competence) which fail to model tissue-like biological response to compound exposures. In this study, HepaRG spheroids were stable and produced highly differentiated functionality for at least 28 days (Supplementary Figure 2C). Therefore, we have initially examined the ability of 3D HepaRG spheroids to model sensitivity of compounds associated (or not associated) with drug-induced liver injury (DILI) (Chen *et al.*, 2011; Xu *et al.*, 2008), and compared these responses with conventional 2D SC-PHHs and 2D HepaRG cells. As shown in Figure 7, aspirin and gemfibrozil were not cytotoxic at any of the concentrations and treatment scenarios examined, consistent with their lack of association with DILI in humans. In contrast, compounds associated with liver injury such as acetaminophen, diclofenac, isoniazid, and cyclosporine A produced marked cytotoxicities. Acetaminophen showed a TC_{50} of approximately 6.1 mM (HepaRG spheroids) and approximately 5.8 mM (PHHs) after 24-h exposures, while repeated exposure of 3D HepaRG spheroids produced significantly more potent response with TC_{50} of approximately 2.9 mM (Figure 7). Similarly, the TC_{50} of diclofenac was 820.2 and approximately 1 mM with 24-h exposures compared with 261.8 μM upon repeated exposure on 3D HepaRG spheroids. Isoniazid and cyclosporine A both produced concentration-related cytotoxicity (>50%) only in HepaRG spheroids with repeated exposure treatments. The TC_{50} of cyclosporine A was 1.9 μM ($P < 0.001$) (Figure 7), which approximated median therapeutic peak plasma concentrations (C_{max}) in human plasma (0.2 μM) upon repeated exposure on HepaRG spheroids. TC_{50} and C_{max} values of other compounds are detailed in Supplementary Table 5.

A useful approach to evaluate the predictivity of *in vitro* approaches for human outcomes is "case study" comparisons with clinically evaluated compounds comparing chemically similar compound analogues which produce highly varied toxicological effects in humans. We compared hepatotoxic compounds trovafloxacin and troglitazone with their "safer" analogues levofloxacin and rosiglitazone in 2D HepaRG, 2D PHHs, and 3D HepaRG spheroids (Figure 7). We observed marked cytotoxicity with trovafloxacin and troglitazone compared with their less toxic analogs levofloxacin and rosiglitazone in 3D HepaRG spheroids with repeated compound exposures over 6 days. TC_{50} of troglitazone and trovafloxacin are 46.2 and 53.01 μM, respectively, which was approximately 10-fold higher than human C_{max} concentrations (Supplementary Table 5).

DISCUSSION

In vitro models which adequately recapitulate the integrated physiological characteristics of native tissues are essential for accurate prediction of chemical-induced adverse effects in humans. Currently, PHHs are considered a "gold standard" for *in vitro* liver models, but their donor-specific variability, finite supply from individual donors, and rapid loss of hepatocyte functionality *in vitro* are major limitations for chemical safety evaluations. Furthermore, immortalized cell lines show poor metabolic competence and biological relevance to liver tissue. A major challenge has been the development of *in vitro* models combining tissue-like functionality, xenobiotic metabolism competency and multiple weeks of longevity in culture with compatibility for higher-throughput screening assays. To overcome these challenges, we have developed and initially characterized a novel 3D *in vitro* liver screening model (384-well format) utilizing HepaRG cells. These 3D liver models undergo morphological and functional differentiation over time to form

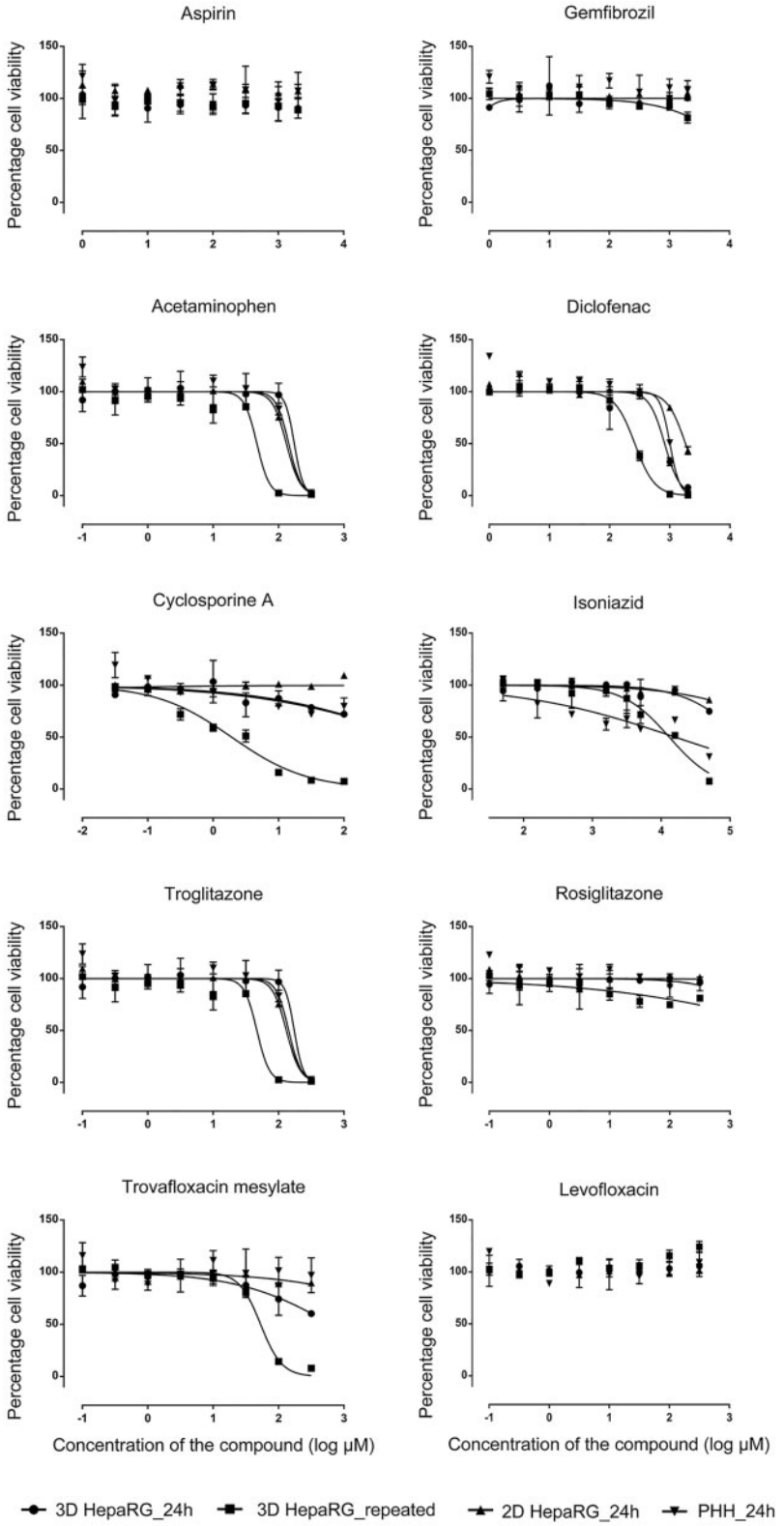

Figure 7. Assessment of chemical induced toxicity. 24-h period single exposures on 2D HepaRG cells cultured for 10 days (▲); 3D HepaRG spheroids cultured for 21 days (•) and primary human hepatocytes cultured for 24 h (▼). Additionally, repeated dosing was performed on 3D HepaRG spheroids at days 22, 24 and 26 (■) and cell viability assessed on day 28. Data are presented as the relative percentage cell viability compared with its vehicle-treated controls. Data are the means of three independent experiments ± SD.

spheroid-like structures which exhibit stable (at least 28 days) hallmarks of hepatocyte functionality including physiologically relevant drug metabolizing activities, liver enzyme inducibility, and evidence of biliary excretion functionality.

When seeded onto 384-well ULA plates, HepaRG cells self-aggregated into a spheroid-like structures. Cell–cell interactions and junctional signaling play a major role in differentiation and maintenance of epithelial cell structure and functionality (Cooper, 2000). The geometry (semi-spherical bottom shape) and low-binding features allowed cells to remain suspended which facilitated cell–cell adhesions and interactions over time resulting in highly differentiated spheroids. HepaRG spheroid formation has been previously described using hanging drop methods (Gunness *et al.*, 2013), spinner bioreactors (Leite *et al.*, 2012), functional polymers (Higuchi *et al.*, 2016). However, unlike other models, the spheroids described here were generated in a simple one-step addition of approximately 1000 cells (no gels, polymers, or spinning) into 384-well plates. This greatly enhanced ease of use, reproducibility/repeatability, reduced potential for compound binding to exogenous ECM, reduced costs, and sufficient throughput for compound screening required for modeling dose- and time-response. One thousand cells per well gave consistent spheroid sizes (approximately 200 μm), while numbers >2000 per well formed "dark" areas in their respective centers consistent with necrotic core formation described previously (Asthana and Kisaalita, 2012) and reduced P450 enzymatic activities (Supplementary Figure 2B).

Differentiated HepaRG spheroids showed polarized cellular morphologies analogous to hepatocytes *in vivo*. MRP2, apical surface marker located at the bile canalicular regions of hepatocytes, is involved in detoxification of xenobiotics and inhibited by various compounds associated with idiosyncratic toxicity (Li *et al.*, 2009; Saab *et al.*, 2013). MRP2 was extensively expressed along the three-dimensional structures of HepaRG spheroids in pockets and channel-like structures Supplementary Movie 3). HepaRG spheroids were also functionally proficient in biliary efflux activity as evidenced by the canalicular localization of synthetic bile acid analogue cholyl-lysyl-fluorescein (CLF). CLF is a fluorescent imaging substrate effectively utilized with rat hepatocytes to study biliary efflux inhibition by drugs and associations with drug-induced liver injury (Barber *et al.*, 2015). Future efforts using this type of image based approach could be extended to HepaRG spheroid models.

HepaRG cells differentiate into hepatocyte- and cholangiocyte-like cell types with approximately 1:1 ratios in 2D cultures (Cerec *et al.*, 2007). In 3D HepaRG spheroids, hepatocytes form the major population, with cholangiocyte-like cells present at apparently reduced proportions, localized at the peripheral regions of the spheroids (Figure 1). These observations are consistent with other reports indicating an enrichment for hepatocyte-like cells in 3D versus 2D configurations (Gunness *et al.*, 2013; Leite *et al.*, 2012), and peripheral cholangiocyte organization in spheroids of PHHs co-cultured with nonparenchymal cells (Bell *et al.*, 2016). Interestingly, some reports with HepaRG spheroids generated with hanging drop and spinner-bioreactor methods have observed localization of cholangiocyte-like cells at the core of aggregates/spheroids (Gunness *et al.*, 2013; Leite *et al.*, 2012). Further studies are required to understand the temporal dynamics of cellular reorganization and differentiation in three-dimensional space, and the impact of biomass, matrices, and culture medium composition on cell signaling mechanisms in 3D tissue models.

An important marker of hepatocyte differentiation is the capacity for xenobiotic metabolism. In this study, we have "benchmarked" pharmacologically important drug metabolizing activities across ranges of interindividual variation observed with suspensions of PHHs reflective of liver tissue levels (and SC-PHH activities). Observed basal enzymatic activities with 3D HepaRG spheroids achieved near-median levels to this benchmark, and far exceeded 2D formats, regardless of the cell type. Previous studies have shown 2D HepaRG cultures under 2% DMSO (Aninat *et al.*, 2006; Cerec *et al.*, 2007; Jackson *et al.*, 2016) approached these levels. However, high DMSO conditions also cause cell death (Nibourg *et al.*, 2012), inhibit toxicologically important CYP2E1, and constitutively induce some P450 expression and limit further inducibility with hepatic receptor activators (Aninat *et al.*, 2006). Not surprisingly, high levels of DMSO during spheroidogenesis resulted in morphological signs of stress during aggregation and were unable to fully form symmetrical/intact spheroids. HepaRG spheroids achieve high levels of metabolic competence without requiring high DMSO concentrations, yet retaining "Zone-2"-like inducibility (Figure 5) in response to prototypical receptor activators (eg AhR, CAR, and PXR). The proprietary "induction" medium additive used in this study was confirmed (personal communication) to contain low levels of DMSO suitable for inducibility studies.

Liver injury in humans at therapeutic doses often requires cumulative exposures to manifest clinical signs (Roberts *et al.*, 2014). HepaRG spheroids maintain physiologically relevant levels of xenobiotic metabolism activity over multiple weeks which enables investigations of repeated exposure scenarios more reflective of human exposures to assess cumulative/slower developing effects (ie liver injury and pharmacology). HepaRG spheroid cultures were, in fact, more responsive to liver injury compounds and metabolically activated toxicants with repeated exposures. Aflatoxin B1 produced increased sensitivity of 3D HepaRG spheroids, which was markedly attenuated by pan-P450 inhibition with 1-ABT. Similar approaches have been reported previously with PHHs (Li, 2009), and liver microsomal mixtures to identify metabolically "activated" toxicants in nonclinical drug discovery (Williams *et al.*, 2003).

A common theme with these initial screening data was a time-dependent progression of hepatocellular injury with compounds associated with metabolically activated toxicity. Acetaminophen was another example of a metabolically activated liver injury compound, producing greater cytotoxicity with repeated exposure in 3D HepaRG approximately 4.7-fold than single exposure 2D HepaRG (approximately 2-fold more potent than single exposures with PHHs). Single exposure acetaminophen with HepaRG spheroids resulted in comparably sensitive TC_{50} (approximately 6.1 mM vs 10.1 mM) relative to previous observations using a hanging drop method (Gunness *et al.*, 2013). Interestingly, Gunness *et al.* (2013) also showed a sensitivity of 2.7 mM with 5-day "old" spheroids. Further evaluations to study the time course of spheroid maturation and potential to simulate developmental tissue states/susceptibilities (eg MRP2 localization, cholangiocyte localization to the periphery after 7 days in 3D culture) may reveal opportunities for modeling both "adult" and "developmental" liver. Cyclosporine A (CsA) was another example of a repeated exposure/time-dependent cytotoxicant with HepaRG spheroids. CsA is primarily metabolized by CYP3A4/5 in humans (Combalbert *et al.*, 1989), and undergoes biliary excretion. Cholestasis was reported in patients taking cyclosporine A (Padda *et al.*, 2011). Further studies to probe the potential for 3D HepaRG spheroids to model cholestasis and the role of uptake and efflux transporters in cyclosporine A-induced damage are warranted.

Two "case study" comparisons of compound analogues with differential liver injury effects in humans were included in this

study: troglitazone versus rosiglitazone, and trovafloxacin versus levofloxacin. Both troglitazone and trovafloxacin were withdrawn from the market due to acute liver failure (Bertino and Fish, 2000; Gale, 2001). With 3D HepaRG spheroids, simple cytotoxicity assays with repeated exposures were effective in discriminating the liver injurious compounds from their "safer" analogs. Interestingly, a previous study reported rosiglitazone-mediated cytotoxicity in HepaRG spheroids (Gunness *et al.*, 2013). Rosiglitazone is generally thought to be less hepatotoxic in humans and remains on the market for anti-diabetic treatment (Floyd *et al.*, 2009; Mendes *et al.*, 2015).The fact that single exposure/time scenarios were less effective in making this distinction is consistent with a time-dependent progression of hepatocellular injury that could have been predicted if these models were available and implemented during drug candidate selection. Diclofenac, troglitazone and trovafloxacin examined in this study have each been reported to be associated with immune mediated idiosyncratic toxicity (Beggs *et al.*, 2015; Edling *et al.*, 2009; Shaw *et al.*, 2009). Even though our model does not have an immune component, the observed cytotoxicity may reveal their initial metabolism mediated cell stress that could eventually lead to overt toxicity. Further improvement of this model with co-cultures of immune cells would help investigating the mechanistic role of inflammation in hepatotoxicity.

In conclusion, this novel HepaRG spheroid model represents a simple one-step approach for obtaining physiologically relevant levels of xenobiotic metabolism and hepatocellular functionality (ie receptor signaling and biliary efflux) in a screening-compatible 384-well format with sufficient longevity and phenotypic stability (at least 28 days) for repeated dose studies. This model exhibits several key cellular architectures of liver tissue, was effective in identifying drug-induced liver injury compounds and distinguishing them from safer "case study" analogues. Further studies are needed to understand the broader complement of tissue functionalities and their utility for toxicological research.

SUPPLEMENTARY DATA

Supplementary data are available at *Toxicological Sciences* online.

ACKNOWLEDGMENTS

We thank Raymond Tice for his leadership to help initiate this research, Alex Merrick for his thoughtful discussions and support, Scott Masten, Masahiko Negishi, and John Bucher for their careful review and suggestions for this manuscript.

FUNDING

This work was supported by the Division of the National Toxicology Program, National Institute of Environmental Health Sciences (NIEHS). This article may be the work product of an employee or group of employees of the NIEHS, NIH; however, the statements contained herein do not necessarily represent the statements, opinions, or conclusions of the NIEHS, NIH of the U.S. Government. The content of this publication does not necessarily reflect the views or the policies of the Department of Health and Human Services nor does mention of trade names, commercial products, or organizations imply endorsement by the U.S. Government.

REFERENCES

Aninat, C., Piton, A., Glaise, D., Le Charpentier, T., Langouet, S., Morel, F., Guguen-Guillouzo, C., and Guillouzo, A. (2006). Expression of cytochromes P450, conjugating enzymes and nuclear receptors in human hepatoma HepaRG cells. *Drug metabolism and disposition: the biological fate of chemicals* **34**(1), 75-83.

Asthana, A., and Kisaalita, W. S. (2012). Microtissue size and hypoxia in HTS with 3D cultures. *Drug Discov Today* **17**(15-16), 810-7.

Barber, J. A., Stahl, S. H., Summers, C., Barrett, G., Park, B. K., Foster, J. R., and Kenna, J. G. (2015). Quantification of Drug-Induced Inhibition of Canalicular Cholyl-l-Lysyl-Fluorescein Excretion From Hepatocytes by High Content Cell Imaging. *Toxicological sciences: an official journal of the Society of Toxicology* **148**(1), 48-59.

Beggs, K. M., Maiuri, A. R., Fullerton, A. M., Poulsen, K. L., Breier, A. B., Ganey, P. E., and Roth, R. A. (2015). Trovafloxacin-induced replication stress sensitizes HepG2 cells to tumor necrosis factor-alpha-induced cytotoxicity mediated by extracellular signal-regulated kinase and ataxia telangiectasia and Rad3-related. *Toxicology* **331**, 35-46.

Bell, C. C., Hendriks, D. F., Moro, S. M., Ellis, E., Walsh, J., Renblom, A., Fredriksson Puigvert, L., Dankers, A. C., Jacobs, F., Snoeys, J., *et al.* (2016). Characterization of primary human hepatocyte spheroids as a model system for drug-induced liver injury, liver function and disease. *Sci Rep* **6**, 25187.

Bertino, J., Jr., and Fish, D. (2000). The safety profile of the fluoroquinolones. *Clinical therapeutics* **22**(7), 798-817; discussion 797.

Cerec, V., Glaise, D., Garnier, D., Morosan, S., Turlin, B., Drenou, B., Gripon, P., Kremsdorf, D., Guguen-Guillouzo, C., and Corlu, A. (2007). Transdifferentiation of hepatocyte-like cells from the human hepatoma HepaRG cell line through bipotent progenitor. *Hepatology* **45**(4), 957-67.

Chen, M., Vijay, V., Shi, Q., Liu, Z., Fang, H., and Tong, W. (2011). FDA-approved drug labeling for the study of drug-induced liver injury. *Drug Discov Today* **16**(15-16), 697-703.

Chu, V., Einolf, H. J., Evers, R., Kumar, G., Moore, D., Ripp, S., Silva, J., Sinha, V., Sinz, M., and Skerjanec, A. (2009). In vitro and in vivo induction of cytochrome p450: a survey of the current practices and recommendations: a pharmaceutical research and manufacturers of america perspective. *Drug Metab Dispos* **37**(7), 1339-54.

Combalbert, J., Fabre, I., Fabre, G., Dalet, I., Derancourt, J., Cano, J. P., and Maurel, P. (1989). Metabolism of cyclosporin A. IV. Purification and identification of the rifampicin-inducible human liver cytochrome P-450 (cyclosporin A oxidase) as a product of P450IIIA gene subfamily. *Drug metabolism and disposition: the biological fate of chemicals* **17**(2), 197-207.

Cooper, G. M. (2000). *The Cell: A Molecular Approach*. 2nd edition ed, Sinauer Associates Inc, Sunderland (MA).

Darnell, M., Schreiter, T., Zeilinger, K., Urbaniak, T., Soderdahl, T., Rossberg, I., Dillner, B., Berg, A. L., Gerlach, J. C., and Andersson, T. B. (2011). Cytochrome P450-dependent metabolism in HepaRG cells cultured in a dynamic three-dimensional bioreactor. *Drug metabolism and disposition: the biological fate of chemicals* **39**(7), 1131-8.

Darnell, M., Ulvestad, M., Ellis, E., Weidolf, L., and Andersson, T. B. (2012). In vitro evaluation of major in vivo drug metabolic pathways using primary human hepatocytes and HepaRG cells in suspension and a dynamic three-dimensional bioreactor system. *J Pharmacol Exp Ther* **343**(1), 134-44.

de Waart, D. R., Hausler, S., Vlaming, M. L., Kunne, C., Hanggi, E., Gruss, H. J., Oude Elferink, R. P., and Stieger, B. (2010). Hepatic transport mechanisms of cholyl-L-lysyl-fluorescein. *The Journal of pharmacology and experimental therapeutics* **334**(1), 78-86.

Edling, Y., Sivertsson, L. K., Butura, A., Ingelman-Sundberg, M., and Ek, M. (2009). Increased sensitivity for troglitazone-induced cytotoxicity using a human in vitro co-culture model. *Toxicol In Vitro* **23**(7), 1387-95.

Elcombe, C. R., Peffer, R. C., Wolf, D. C., Bailey, J., Bars, R., Bell, D., Cattley, R. C., Ferguson, S. S., Geter, D., Goetz, A., *et al*. (2014). Mode of action and human relevance analysis for nuclear receptor-mediated liver toxicity: A case study with phenobarbital as a model constitutive androstane receptor (CAR) activator. *Crit Rev Toxicol* **44**(1), 64-82.

Floyd, J. S., Barbehenn, E., Lurie, P., and Wolfe, S. M. (2009). Case series of liver failure associated with rosiglitazone and pioglitazone. *Pharmacoepidemiol Drug Saf* **18**(12), 1238-43.

Gale, E. A. (2001). Lessons from the glitazones: a story of drug development. *Lancet* **357**(9271), 1870-5.

Gallagher, E. P., Kunze, K. L., Stapleton, P. L., and Eaton, D. L. (1996). The kinetics of aflatoxin B1 oxidation by human cDNA-expressed and human liver microsomal cytochromes P450?1A2 and 3A4. *Toxicol Appl Pharmacol* **141**(2), 595-606.

Gripon, P., Rumin, S., Urban, S., Le Seyec, J., Glaise, D., Cannie, I., Guyomard, C., Lucas, J., Trepo, C., and Guguen-Guillouzo, C. (2002). Infection of a human hepatoma cell line by hepatitis B virus. *Proc Natl Acad Sci U S A* **99**(24), 15655-60.

Guillouzo, A., Corlu, A., Aninat, C., Glaise, D., Morel, F., and Guguen-Guillouzo, C. (2007). The human hepatoma HepaRG cells: a highly differentiated model for studies of liver metabolism and toxicity of xenobiotics. *Chem Biol Interact* **168**(1), 66-73.

Gunness, P., Mueller, D., Shevchenko, V., Heinzle, E., Ingelman-Sundberg, M., and Noor, F. (2013). 3D organotypic cultures of human HepaRG cells: a tool for in vitro toxicity studies. *Toxicol Sci* **133**(1), 67-78.

Guo, L., Dial, S., Shi, L., Branham, W., Liu, J., Fang, J. L., Green, B., Deng, H., Kaput, J., and Ning, B. (2011). Similarities and differences in the expression of drug-metabolizing enzymes between human hepatic cell lines and primary human hepatocytes. *Drug metabolism and disposition: the biological fate of chemicals* **39**(3), 528-38.

Hariparsad, N., Carr, B. A., Evers, R., and Chu, X. (2008). Comparison of immortalized Fa2N-4 cells and human hepatocytes as in vitro models for cytochrome P450 induction. *Drug metabolism and disposition: the biological fate of chemicals* **36**(6), 1046-55.

Higuchi, Y., Kawai, K., Kanaki, T., Yamazaki, H., Chesne, C., Guguen-Guillouzo, C., and Suemizu, H. (2016). Functional polymer-dependent 3D culture accelerates the differentiation of HepaRG cells into mature hepatocytes. *Hepatol Res* doi: 10.1111/hepr.12644.

Jackson, J. P., Li, L., Chamberlain, E. D., Wang, H., and Ferguson, S. S. (2016). Contextualizing Hepatocyte Functionality of Cryopreserved HepaRG Cell Cultures. *Drug metabolism and disposition: the biological fate of chemicals* **44**(9), 1463-79.

Kang, S. J., Lee, H. M., Park, Y. I., Yi, H., Lee, H., So, B., Song, J. Y., and Kang, H. G. (2016). Chemically induced hepatotoxicity in human stem cell-induced hepatocytes compared with primary hepatocytes and HepG2. *Cell Biol Toxicol* **32**(5), 403-17.

Khetani, S. R., Kanchagar, C., Ukairo, O., Krzyzewski, S., Moore, A., Shi, J., Aoyama, S., Aleo, M., and Will, Y. (2013). Use of micropatterned cocultures to detect compounds that cause drug-induced liver injury in humans. *Toxicol Sci* **132**(1), 107-17.

Kullak-Ublick, G. A., Baretton, G. B., Oswald, M., Renner, E. L., Paumgartner, G., and Beuers, U. (2002). Expression of the hepatocyte canalicular multidrug resistance protein (MRP2) in primary biliary cirrhosis. *Hepatol Res* **23**(1), 78-82.

Leite, S. B., Wilk-Zasadna, I., Zaldivar, J. M., Airola, E., Reis-Fernandes, M. A., Mennecozzi, M., Guguen-Guillouzo, C., Chesne, C., Guillou, C., Alves, P. M., *et al*. (2012). Three-dimensional HepaRG model as an attractive tool for toxicity testing. *Toxicol Sci* **130**(1), 106-16.

Levine, J. F., and Stockdale, F. E. (1985). Cell-cell interactions promote mammary epithelial cell differentiation. *J Cell Biol* **100**(5), 1415-22.

Levy, G., Bomze, D., Heinz, S., Ramachandran, S. D., Noerenberg, A., Cohen, M., Shibolet, O., Sklan, E., Braspenning, J., and Nahmias, Y. (2015). Long-term culture and expansion of primary human hepatocytes. *Nature biotechnology* **33**(12), 1264-1271.

Li, A. P. (2009). Metabolism Comparative Cytotoxicity Assay (MCCA) and Cytotoxic Metabolic Pathway Identification Assay (CMPIA) with cryopreserved human hepatocytes for the evaluation of metabolism-based cytotoxicity in vitro: proof-of-concept study with aflatoxin B1. *Chemico-biological interactions* **179**(1), 4-8.

Li, N., Zhang, Y., Hua, F., and Lai, Y. (2009). Absolute difference of hepatobiliary transporter multidrug resistance-associated protein (MRP2/Mrp2) in liver tissues and isolated hepatocytes from rat, dog, monkey, and human. *Drug metabolism and disposition: the biological fate of chemicals* **37**(1), 66-73.

Linder, C. D., Renaud, N. A., and Hutzler, J. M. (2009). Is 1-aminobenzotriazole an appropriate in vitro tool as a nonspecific cytochrome P450 inactivator? *Drug metabolism and disposition: the biological fate of chemicals* **37**(1), 10-3.

Mendes, D., Alves, C., and Batel-Marques, F. (2015). Number needed to harm in the post-marketing safety evaluation: results for rosiglitazone and pioglitazone. *Pharmacoepidemiol Drug Saf* **24**(12), 1259-70.

Mueller, D., Kramer, L., Hoffmann, E., Klein, S., and Noor, F. (2014). 3D organotypic HepaRG cultures as in vitro model for acute and repeated dose toxicity studies. *Toxicol In Vitro* **28**(1), 104-12.

Nguyen, D. G., Funk, J., Robbins, J. B., Crogan-Grundy, C., Presnell, S. C., Singer, T., and Roth, A. B. (2016). Bioprinted 3D Primary Liver Tissues Allow Assessment of Organ-Level Response to Clinical Drug Induced Toxicity In Vitro. *PLoS One* **11**(7), e0158674.

Nibourg, G. A., Chamuleau, R. A., van der Hoeven, T. V., Maas, M. A., Ruiter, A. F., Lamers, W. H., Oude Elferink, R. P., van Gulik, T. M., and Hoekstra, R. (2012). Liver progenitor cell line HepaRG differentiated in a bioartificial liver effectively supplies liver support to rats with acute liver failure. *PLoS One* **7**(6), e38778.

Novik, E., Maguire, T. J., Chao, P., Cheng, K. C., and Yarmush, M. L. (2010). A microfluidic hepatic coculture platform for cell-based drug metabolism studies. *Biochem Pharmacol* **79**(7), 1036-44.

Ostapowicz, G., Fontana, R. J., Schiodt, F. V., Larson, A., Davern, T. J., Han, S. H., McCashland, T. M., Shakil, A. O., Hay, J. E., Hynan, L., *et al*. (2002). Results of a prospective study of acute liver failure at 17 tertiary care centers in the United States. *Annals of internal medicine* **137**(12), 947-54.

Padda, M. S., Sanchez, M., Akhtar, A. J., and Boyer, J. L. (2011). Drug-induced cholestasis. *Hepatology* **53**(4), 1377-87.

Parkinson, A. (1996). An overview of current cytochrome P450 technology for assessing the safety and efficacy of new materials. *Toxicol Pathol* **24**(1), 48-57.

Ramaiahgari, S. C., den Braver, M. W., Herpers, B., Terpstra, V., Commandeur, J. N., van de Water, B., and Price, L. S. (2014). A 3D in vitro model of differentiated HepG2 cell spheroids with improved liver-like properties for repeated dose high-throughput toxicity studies. *Arch Toxicol* **88**(5), 1083-95.

Roberts, R. A., Kavanagh, S. L., Mellor, H. R., Pollard, C. E., Robinson, S., and Platz, S. J. (2014). Reducing attrition in drug development: smart loading preclinical safety assessment. *Drug Discov Today* **19**(3), 341-7.

Saab, L., Peluso, J., Muller, C. D., and Ubeaud-Sequier, G. (2013). Implication of hepatic transporters (MDR1 and MRP2) in inflammation-associated idiosyncratic drug-induced hepatotoxicity investigated by microvolume cytometry. *Cytometry A* **83**(4), 403-8.

Shaw, P. J., Beggs, K. M., Sparkenbaugh, E. M., Dugan, C. M., Ganey, P. E., and Roth, R. A. (2009). Trovafloxacin enhances TNF-induced inflammatory stress and cell death signaling and reduces TNF clearance in a murine model of idiosyncratic hepatotoxicity. *Toxicol Sci* **111**(2), 288-301.

Treyer, A., and Musch, A. (2013). Hepatocyte polarity. *Compr Physiol* **3**(1), 243-87.

Walsky, R. L., and Obach, R. S. (2004). Validated assays for human cytochrome P450 activities. *Drug metabolism and disposition: the biological fate of chemicals* **32**(6), 647-60.

Wild, C. P., and Turner, P. C. (2002). The toxicology of aflatoxins as a basis for public health decisions. *Mutagenesis* **17**(6), 471-81.

Williams, J. A., Hurst, S. I., Bauman, J., Jones, B. C., Hyland, R., Gibbs, J. P., Obach, R. S., and Ball, S. E. (2003). Reaction phenotyping in drug discovery: moving forward with confidence? *Curr Drug Metab* **4**(6), 527-34.

Wong, N., Lai, P., Pang, E., Leung, T. W., Lau, J. W., and Johnson, P. J. (2000). A comprehensive karyotypic study on human hepatocellular carcinoma by spectral karyotyping. *Hepatology* **32**(5), 1060-8.

Xu, J. J., Henstock, P. V., Dunn, M. C., Smith, A. R., Chabot, J. R., and de Graaf, D. (2008). Cellular imaging predictions of clinical drug-induced liver injury. *Toxicol Sci* **105**(1), 97-105.

Yamada, K. M., and Cukierman, E. (2007). Modeling tissue morphogenesis and cancer in 3D. *Cell* **130**(4), 601-10.

Zanger, U. M., and Schwab, M. (2013). Cytochrome P450 enzymes in drug metabolism: regulation of gene expression, enzyme activities, and impact of genetic variation. *Pharmacology & therapeutics* **138**(1), 103-41.

Zhang, J. G., Ho, T., Callendrello, A. L., Clark, R. J., Santone, E. A., Kinsman, S., Xiao, D., Fox, L. G., Einolf, H. J., and Stresser, D. M. (2014). Evaluation of calibration curve-based approaches to predict clinical inducers and noninducers of CYP3A4 with plated human hepatocytes. *Drug metabolism and disposition: the biological fate of chemicals* **42**(9), 1379-91.